HHS Public Access

Author manuscript

Obesity (Silver Spring). Author manuscript; available in PMC 2018 April 25.

Published in final edited form as:

Obesity (Silver Spring). 2017 December ; 25(12): 2079–2087. doi:10.1002/oby.21980.

Intramyocellular Lipid Droplet Size Rather Than Total Lipid Content Is Related to Insulin Sensitivity After 8-Weeks of Overfeeding

Jeffrey D. Covington[1,2], **Darcy L. Johannsen**[1], **Paul M. Coen**[3], **David H. Burk**[1], **Diana N. Obanda**[1], **Philip J. Ebenezer**[1], **Charmaine S. Tam**[5], **Bret H. Goodpaster**[3], **Eric Ravussin**[1], and **Sudip Bajpeyi**[1,4]

[1]Pennington Biomedical Research Center, Laboratory of Skeletal Muscle Physiology, 6400 Perkins Road, Baton Rouge, LA 70808

[2]Louisiana State University Health Sciences Center, School of Medicine, 433 Bolivar St, New Orleans, LA 70112

[3]Translational Research Institute for Metabolism and Diabetes Florida Hospital • Sanford-Burnham Medical Research Institute, 301 East Princeton Street, Orlando, FL 32804

[4]Universtiy of Texas at El Paso, Department of Kinesiology, 500 University Ave, El Paso, TX, 79968

[5]The Charles Perkins Centre and The School of Biological Sciences, University of Sydney, NSW, Australia

Abstract

Objective—Intramyocellular lipid (IMCL) is inversely related to insulin sensitivity in sedentary populations, yet no prospective studies in humans have examined IMCL accumulation with overfeeding.

Methods—Twenty-nine males were overfed a high-fat diet (140% caloric intake, 44% from fat) for 8-weeks. Measures of IMCL, whole body fat oxidation from a 24-hour metabolic chamber, muscle protein extracts, and muscle ceramide measures were obtained before and after the intervention.

Corresponding Author: Sudip Bajpeyi, PhD, Assistant Professor, Department of Kinesiology, University of Texas at El Paso, 500 University Ave; El Paso, TX 79968, Phone: 915-747-5461, sbajpeyi@utep.edu.

J.D.C. conceived the experiment, performed experiments, analyzed data, and wrote the manuscript; D.L.J. contributed to discussion and reviewed/edited the manuscript; P.M.C. performed experiments and reviewed/edited the manuscript; D.H.B. contributed to discussion and reviewed/edited the manuscript; D.N.O. performed experiments and reviewed/edited the manuscript; P.E. performed experiments and reviewed/edited the manuscript; C.S.T. contributed to discussion and reviewed/edited the manuscript; B.H.G. contributed to discussion and reviewed/edited the manuscript; E.R. contributed to the discussion, conceived of the experiment, and reviewed/edited the manuscript; S.B. contributed to the discussion, conceived the experiment, and reviewed/edited the manuscript. All authors gave final approval of the manuscript prior to submission. J.D.C. is the guarantor of this work, and, as such, had full access to all the data in the study and takes responsibility for the integrity of the data and the accuracy of the data analysis.

Conflict of Interest Statement: The authors have no competing interests.

clinicaltrials.gov identifier: NCT01672632; URL: NCT01672632https://clinicaltrials.gov/ct2/show/NCT01672632?term=NCT01672632&rank=1

Results—Eight weeks of overfeeding did not increase overall IMCL. The content of smaller lipid droplets peripherally located in the myofiber decreased while increases in larger droplets correlated inversely to glucose disposal rate. Overfeeding resulted in inhibition of Akt activity, which correlated with the reductions in smaller, peripherally located lipid droplets and to drastic increases in ceramide content. Additionally, peripherally located lipid droplets were associated with more efficient lipid oxidation. Finally, participants, who maintained more smaller, peripherally located lipid droplets, displayed a better resistance to weight gain with overfeeding.

Conclusions—These results show that lipid droplet size and location rather than mere IMCL content is important to understanding insulin sensitivity.

Keywords

Ectopic Lipid; Myotube; PAT protein; Perilipin 3; Perilipin 2; Type 2 Diabetes; Obesity

Introduction

Type 2 diabetes (T2D) is a condition diagnostically characterized by hyperglycemia with insulin resistance being an early pathological insult. Repeatedly, studies have provided evidence that higher levels of intramyocellular lipid (IMCL) in non-diabetic insulin sensitive and insulin resistant patients are inversely related to insulin sensitivity (1). The exact mechanisms behind this relationship are not fully understood, but much research has been directed at this phenomenon.

To further complicate this relationship, endurance trained athletes, who are highly insulin sensitive, also possess large quantities of IMCL (2). Similarly, we have previously shown that human primary myotubes collected from physically active, insulin sensitive donors also have a greater IMCL content compared to myotubes collected from less insulin sensitive, sedentary individuals of similar body weight (3). In addition, longitudinal exercise training studies, which have long been known to improve insulin sensitivity, have not resulted in a consistent effect on IMCL content. Exercise training has been shown to increase (4), not change (5), or even a decrease in IMCL content (6). As exercise training and physical activity have a powerful impact on several physiological systems, it is difficult to use an exercise training model to thoroughly understand the relationship between IMCL accumulation and insulin resistance that is clearly established in a sedentary population such as obesity and type 2 diabetes.

Prior studies have utilized experimental interventions of isocaloric high fat diet (7), intravenous lipid infusions (8), and overfeeding (9). Since the obesogenic western diet is associated with weight gain, insulin resistance, and a higher prevalence of obesity (10), the overfeeding experimental paradigm appears to be the best way to test the mechanisms underlying the deleterious effects of western diets (11). We, therefore, endeavored to overfeed 29 healthy male participants a high fat diet (140% of nutritional calories provided compared to resting metabolic rate; 44% macronutrient content from fat) for 8 weeks and found significant weight gain and reductions in insulin sensitivity (12). Given this, we explored alterations in IMCL content from three muscles: the soleus, the tibialis anterior, and the vastus lateralis.

Methods and Procedures

Participant recruitment and study design

We recruited 29 male participants (age: 26.8 ± 5.4 yrs; BMI: 25.5 ± 2.3 kg/m^2). All participants provided informed consent, and study parameters were approved by the Institutional Review Board of Pennington Biomedical Research Center. Our study was registered on clinicaltrials.gov (clinicaltrials.gov identifier: NCT01672632). Prior to the 8-week overfeeding period, participants completed a 14-day measurement of free-living energy expenditure by doubly labeled water (DLW) (13) to determine baseline energy requirements. Additionally, physical activity levels were assessed using tri-axial accelerometers during that time period. During the second week of DLW participants consumed an isocaloric diet (60% carbohydrate, 25% fat, 15% protein). Participants then underwent baseline clinical procedures; the same clinical measures were also conducted after 8 weeks of overfeeding. Following baseline measures, participants consumed a diet for the next 8-weeks of 44% fat, 15% protein, and 41% carbohydrate, where the total daily intake equated to 140% of their normal caloric intake to maintain body weight. Glucose disposal rate (GDR) was determined using a euglycemic-hyperinsulinemic clamp with a insulin infusion of 50mU/min/m^2, and adjusted for fat free mass (FFM) +17.7, denoted as estimated mean body size (EMBS), as previously described (14). Metabolic respiratory measures of 24-hour respiratory quotient (RQ), Sleep RQ, and non-protein RQ were conducted in a 24-hour metabolic chamber as previously described (15). Serum measures were assessed in a certified clinical chemistry laboratory and were performed by enzymatic assays on a Beckman Coulter DXC 600 (Beckman Coulter, Brea, CA). Body composition was assessed by dual x-ray absorptiometry (DXA, QDR 4500A; Hologics, Bedford, MA), and MRI (3.0 T magnet; Excite HD Systems; General Electirc; Milwaukee, WI).

Skeletal Muscle Biopsy Procedure

After an overnight fast, skeletal muscle samples were collected using the Bergstrom technique with suction from the vastus lateralis (Propper Manufacturing Co., Long Island City, NY), following administration of local anesthetic of lidocaine/bupivacaine. Samples for ceramide content, mRNA and protein measures were immediately snap frozen in liquid nitrogen. A sample for immunohistochemical measures of vastus lateralis intramyocellular lipid, lipid droplet size quantification, and fiber typing was blotted dry and then mounted in Optimal Cutting Temperature (OCT, Thermo Scientific, Waltham, MA) and frozen in isopentane cooled over liquid nitrogen. Other samples were collected for measurements of *ex vivo* palmitate oxidation, mitochondrial extraction, and a final sample was placed in a solution of DMEM and 1% Pen/strep at 5mg/mL (Life Technologies, Grand Island, NY) for establishment of primary skeletal muscle cultures. Primary muscle cultures were established from muscle biopsies obtained from five donors (Age 23.0±1.9yrs and BMI 24.2±0.6kg/m^2) at baseline of this study. Establishment of human primary muscle culture has been modified from protocols as previously described (16), and cultures from the five donors were grown simultaneously to approximately 90% confluence and then pooled together for experiments using protocols previously described (17).

Ex vivo Palmitate Oxidation Measures in Skeletal Muscle

Approximately 75 mg of skeletal muscle tissue was homogenized and loaded into a trapping plate apparatus to assess gas exchange for fatty acid oxidation. 0.176 μM of total palmitate (0.088 μM of [1-^{14}C]-palmitate in 0.088 μM of non-radiolabeled palmitate) was added to the muscle homogenate. Radiolabeled palmitate was obtained from American Radiolabeled Chemicals (St. Louis, MO). Radiolabeled $^{14}CO_2$ and incomplete acid soluble intermediates from palmitate oxidation were assessed using scintillation counting. Data was adjusted to total protein content obtained from muscle homogenate as determined through the bicinchoninic acid assay (Pierce BCA, Thermo Scientific, Waltham, MA).

Immunohistochemical Measures in Vastus Lateralis

Serial transverse sections (10μm) of mounted biopsy samples were generated using a cryostat (Cryotome E; Thermo Shandon, Pittsburgh, PA) at -20°C and placed on slides (Fisherfinest, Fischer Scientific, Pittsburgh, PA). Sections were then stained in a filtered solution of Oil Red O (300mg/ml in 36% triethylphosphate) for 30 minutes at room temperature. Thereafter, sections were incubated with primary antibodies for anti-human myosin heavy chain (MYH)7 (type I myocytes) and MYH2 (type IIa myocytes) overnight at room temperature and subsequently incubated with fluorescein (FITC) (type IIa myocytes) and Rhodamine (type I myocytes) conjugated secondary antibodies (Santa Cruz Biotechnologies, Santa Cruz, CA). Type IIx fibers remained unstained. Images were visualized using a Leica microscope (Leica DM 4000B; Leica Microsystems, Bannockburn, IL), digitally captured (Retiga 2000R camera; Q Imaging, Surrey, Canada), and IMCL was analyzed using specialized software (Northern Eclipse, v6.0; Empix Imaging, Cheektowaga, NY). Fiber type was determined by counting the total number of fibers and assessing the percentage of those positive for MYH7 and MYH2.

Mitochondrial ROS Production

Mitochondrial reactive oxygen species (ROS) production was measured from methods adapted from Seifert et al. (18) Briefly, mitochondrial were extracted from 200mg of muscle tissue using the methods of Chappelle and Perry (19, 20) and suspended in an incubation media containing 120mM KCl, 5mM KH_2PO_4, 3mM Hepes, 1mM EGTA, and 0.3% BSA (pH 7.4). Mitochondria were then infused with palmitoyl carnitine (60μM), and ROS production was accessed fluorimetrically as a rate of H_2O_2 emission using p-hydroxyphenylacetate (PHPA; 167μg/mL) and horseradish peroxidase (9 units/mL) in mitochondria suspended in incubation media. H_2O_2 emission was monitored for 25 mins at 37°C in a fluorimeter at an excitation of 320nm and emission of 400nm.

Protein Expression

Total protein for all experiments was collected using RIPA buffer (Sigma, St. Louis, MO) supplemented with 2% Protease Inhibitor Cocktail (Sigma, St. Louis, MO), 2% Phosphatase Inhibitor Cocktail 2 (Sigma, St. Louis, MO), and 2% Phosphatase Inhibitor Cocktail 3 (Sigma, St. Louis, MO). Protein content was assessed from total protein extracts using western immunoblotting with the Criterion apparatus system using 4-15% SDS-polyacrylamide gradient gels (all from Bio-Rad, Hercules, CA) and adjusted to GAPDH

(Cat no. AB9484; AbCam, Cambrige, MA). Imaging of western blots was facilitated on the Odyssey infrared imaging system (LiCor, Lincoln, Nebraska). Antibodies against Total Akt (Cat no. 9272), p-S473 Akt (Cat no. 9271), Total IRS1 (Cat no. 2382S), p-S1101 IRS1 (Cat no. 2385), and mTOR (Cat no. 4517) were obtained from Cell Signaling Technology (Danvers, MA) The antibodies for PLIN2 (Cat no. NB110-40877) and PLIN3 (Cat no. NB110-40764) were obtained from Novus Biologicals (Littleton, CO).

Lipid droplet quantification within skeletal muscle

Lipid droplet quantification was obtained using greyscale images of ORO stained muscle sections minimally processed in FIJI (21) through background subtraction using empirically derived background images. Regions of interest (ROI) representing individual muscle fibers were manually drawn, and the central and peripherial (band) ROIs were generated using the 'Enlarge' and 'Make Band' tools within FIJI. Lipid droplet counts and size distribution data were determined by using the 'Analyze Particles' tool with a size exclusion of 2-70 pixels and circularity filter setting of 0.5–1.00.

Ceramide Measures in Skeletal Muscle

Ceramide was measured using double extraction for lipids using 50mg of skeletal muscle biopsy tissue and processed as previously shown (22). Liquid chromatography-electrospray ionization tandem-mass spectrometry was used to quantify ceramides as previously described (22). According to the retention times of standards, common product ions and ions reflecting fatty acid substituents, all target ceramide species were quantified.

Limitations to measures

Due to the rigorous requirements by study participants for performing an overfeeding paradigm and also to limitations is skeletal muscle biopsy material, it was impossible to obtain a complete data set for every data point measured in our study. Even though we recruited 29 participants, we were only able to obtain lipid droplet quantification on 25 participants. Additionally, certain procedures that required large quantities of biopsy material (*ex vivo* palmitate oxidation and *ex vivo* mitochondrial isolation for ROS generation) were only obtained on a subset of our participants.

Statistical Analysis

Data were analyzed using PRISM GraphPad Software, version 6.0 (GraphPad Software, La Jolla, CA). All data were determined to be normally distributed using the Shapiro-Wilk normality test. Data that were normally distributed was analyzed using parametric methods (Person r correlation coefficients and paired, two-way t-tests), while data not normally distributed were analyzed using non-parametric methods (Spearman rho correlation coefficients and Wilcoxon signed ranked paired tests). A p value ≤ 0.05 was considered statistically significant. All graphs are represented as mean±S.E.M.

Results

Eight Weeks of Overfeeding Altered Lipid Droplet Size and Location

Eight weeks of overfeeding in 29 males resulted in weight gain, an increase in percent fat accumulation, but only a trend towards a decrease in insulin sensitivity (Table 1). Furthermore, there were no significant changes observed in the total content of IMCL in three separate muscles: soleus, tibilais antertior, or vastus lateralis (Figure 1A), nor were there differences in the fiber type specific content of IMCL in vastus lateralis (Figure 1B). However, we found significant reductions in the content of smaller sized lipid droplets around the periphery of the myofiber (p=0.005, Figure 1C), and trends towards reductions in the whole myofiber (p=0.07, Figure S1A) and centrally located lipid droplets (p=0.09, Figure S1B). Glucose disposal rate (GDR) was inversely associated with the content of larger lipid droplets in the whole myofiber (r=-0.47, p=0.02, Figure 1E) and centrally located lipid droplets (r=-0.60, p=0.008, Figure S1C).

Changes in Smaller Lipid Droplets were Associated with Less ROS Generation from Lipid Oxidation and Different Lipid Associated Proteins

Associations between lipid oxidation and lipid droplet size/localization were examined, and we found that baseline levels of smaller, peripherally located lipid droplets were associated with whole body lipid oxidation as indicated by the inverse trends with 24-hour respiratory quotient (RQ, r=-0.35, p=0.09, N=24, Figure 2A) and a significant inverse relationship with sleep RQ (r=-0.57, p=0.004, N=24, Figure 2B). Changes with overfeeding showed decreases in the content of smaller lipid droplets trended towards an association with increases in whole body lipid oxidation (r=0.38, p=0.07, N=24, Figure 2C) as well as significantly related to *ex vivo* lipid oxidation from the vastus lateralis muscle (r=-0.58, p=0.04, N=12, Figure 2D). Importantly, the production of ROS from palmitoyl-carnitine (PC) using extracted mitochondria from the vastus lateralis revealed a pre-intervention relationship between levels of PC induced ROS production and smaller, peripherally located lipid droplets (r=-0.72, p=0.01, N=11, Figure 2E). Additionally, the retention of smaller, peripherally located lipid droplets with overfeeding was associated with less PC induced ROS production (r=-0.62, p=0.04, N=11, Figure 2F).

Given the decline in smaller lipid droplets in our study and prior studies indicating that Perilipin 2 (PLIN2 and Perilipin 3 (PLIN3) are associated with larger and smaller lipid droplet sizes respectively (23), we report a significant decrease in PLIN3 protein with overfeeding (p=0.04, Figure 3A) and no change in PLIN2 protein content (data not shown). Using primary myotubes cultured from the donors from this study, we show that the increase in PLIN2 protein is dependent on incubation time (200μM Palmitate, Figure 3B). In relation to this, we found a correlation between changes in PLIN2 protein content in skeletal muscle and the decrease in smaller, peripherally located lipid droplets (r=-0.48, p=0.02, data not shown). Importantly, there was an inverse correlation between changes in PLIN2 protein content and changes in GDR (r=-0.43, p=0.03; Figure 3C).

Smaller Lipid Droplet Depletion Was Associated with Reduced Akt Phosphorylation and Increased Ceramides

To understand the mechanisms responsible for the interaction between glucose disposal and lipid droplet redistribution, we found a significant reduction in the phosphorylation of Akt at S473 (p=0.05, Figure 4A) after overfeeding, which was associated with the depletion of smaller, peripherally located lipid droplets (r=0.47, p=0.04, data not shown). There were no differences in the phosphorylation of IRS1 at S1101 (data not shown). Given that a high ceramide content has been shown to reduce Akt phosphorylation independent of altering other aspects of the insulin signaling cascade (24), we measured the muscle content of ceramides and found it to be increased with overfeeding (p<0.001, Figure 4B) regardless of the subspecies (Figure 4C). Ceramide content was inversely related to S473-Akt phosphylation (r=-0.47, p=0.04, Figure 4D). In addition, mTOR protein content increased in skeletal muscle with overfeeding (p=0.05, Figure 4E).

Retention of Smaller Lipid Droplets is Associated with Higher Physical Activity and Resistance to Weight Gain Induced with Overfeeding

Prospectively, we found that those with higher baseline physical activity levels (PAL, r=0.64, p=0.002), higher metabolic equivalents (METs, r=0.47, p=0.03), and higher total daily energy expenditure (TDEE, r=0.50, p=0.01) were relatively protected against a decrease in smaller, peripherally located lipid droplets in response to 8 weeks of overfeeding. Importantly, participants with higher levels of smaller, peripheral lipid droplets, were also more resistant to weight gain during overfeeding (r=-0.44, p=0.03, Figure 5).

Discussion

Our study highlights for the first time that prospective examination of intramyocellular lipid content, on average, does not change with eight weeks of high-fat diet overfeeding. The participants of this study gained 7.6kg on average over the eight-week period and thus our original hypothesis was that overfeeding would result in increased IMCL. Surprisingly, there were no differences in IMCL measured in soleus, tibialis anterior, and vastus lateralis muscles (Figure 1A) regardless of fiber type examined in the vastus lateralis (Figure 1B). These results led us to investigate how alterations in lipid organization within muscle might influence insulin sensitivity.

IMCL is stored in the form of lipid droplets, thus implicating lipid droplet size and subcellular localization to be important in understanding skeletal muscle insulin resistance. Prior reports have shown reductions in lipid droplet size with weight loss associated with increased insulin sensitivity (25). Subcellular localization of lipid droplets has been shown to be different based on physically activity with highly active individuals having more lipid droplets around the periphery of the myofiber (26). Furthermore, stimulated contraction of muscle shows a preference for depleting lipid droplets around the outer bands of the myofiber with increased lipid oxidation (27). These insights led us to hypothesize that overfeeding would result in a reduction in the content of smaller, peripherally located lipid droplets, and that these reductions would be associated with worsening in insulin sensitivity. Indeed, there were significant reductions in the content of smaller sized lipid droplets around

the periphery of the myofiber (Figure 1B), as well as trends towards reductions of both centrally located lipid droplets (Figure S1A) and globally throughout the whole myofiber (Figure S1B). Our present study highlights a relationship between the change in glucose infusion rates with the change in the content of larger lipid droplets in the whole myofiber (Figure 1E) and centrally located lipid droplets (Figure S1C).

To understand the mechanisms responsible for the interaction between glucose infusion rates and lipid droplets redistribution, we first examined the canonical insulin signaling pathway, which showed a significant reduction in the phosphorylation of Akt-S473 (Figure 2A), but not phosphorylation of IRS1- S1101. Given this observation, we aimed specifically to understand why Akt might be altered without changes in IRS1 and focused on ceramide targets that are known to disrupt insulin signaling at the Akt level independent of altering other aspects of the signaling cascade (24). Additionally, studies in humans have shown that increased ceramide content in muscle is associated with insulin resistance (28). Our study did show that ceramide content significantly increased in muscle following overfeeding (Figure 2B and 2C); however, it should also be noted that though the average levels of ceramides increased significantly, insulin sensitivity only trended towards a decrease (Table 1). Ceramide content, though, was inversely related to S473-Akt phosphylation (Figure 2D). Given recent investigations implicating mTOR signaling in ceramide induced inhibition of Akt activity (29), we investigated levels of mTOR and found a significant increase in mTOR protein content (Figure 2E) after overfeeding. Based on these results, we postulate that increases in intramyocellular ceramide content were responsible for the inhibition of insulin signaling. In addition since smaller, peripherally located lipid droplets are preferentially oxidized (27), we speculate that the depletion of these lipid droplets would be linked to either reductions in lipid oxidation, inefficiencies in lipid oxidation, or both, which in turn would contribute to the accumulation in ceramide content.

Isoenergetic high fat consumption has been shown to increase lipid oxidation (30), and thus we examined any associations between lipid oxidation and lipid droplet size/localization. Baseline levels of smaller, peripherally located lipid droplets were associated with whole body lipid oxidation as indicated by the inverse correlations with sleep RQ. However, we found that decreases in the content of smaller lipid droplets after overfeeding were associated with increased whole body lipid oxidation as well as *ex vivo* lipid oxidation in vastus lateralis muscle. In connection to this, an increase in lipid oxidation after the high fat diet is often incomplete resulting in the production of oxidative lipotoxic species (31, 32), and smaller lipid droplets is more so associated with less lipotoxic fat oxidation. To explore this further, we measured the production of reactive oxygen species (ROS) from palmitoyl-carnitine (PC) using extracted mitochondria from the vastus lateralis and found that pre-intervention levels of PC induced ROS production were inversely associated with smaller, peripherally located lipid droplets. Additionally, the retention of smaller, peripherally located lipid droplets with overfeeding was associated with less PC induced ROS production suggesting that smaller, peripherally located lipid droplets produce more efficient, less lipotoxic oxidation with overfeeding.

In order to further understand connections between lipid droplet size and lipid oxidation, we examined the alterations in key lipid droplet associated proteins within the skeletal muscle.

Lipid droplet associated proteins (particularly the perilipin family (23)) have been shown to coat lipid droplets based on their size (33) and have also been shown to play a role in lipid oxidation. Recently, we have shown that PLIN3 is positively associated with both whole body *in vivo* and skeletal muscle *ex vivo* lipid oxidation (34). Given our study shows a decline in smaller lipid droplets after overfeeding and prior studies showing an association between PLIN3 and smaller lipid droplets (23), a significant decrease in PLIN3 protein content with overfeeding (Figure 3A) is in line with present literature. Additionally, the expression of PLIN2 is associated with larger lipid droplets (23). Though prior studies have shown PLIN2 to become expressed with increasing duration of lipid incubation using mice and mouse cell lines (35), we show for the first time using primary myotubes cultured from the donors from this study that the increase in PLIN2 protein is dependent on incubation time (200μM Palmitate, Figure 3B). Based on these data, we speculate that as smaller lipid droplets were being depleted, perhaps lipid droplets that remained were being packaged with PLIN2. Though we did not see a change in PLIN2 protein content with overfeeding, we saw an inverse correlation between a decrease in smaller, peripherally located lipid droplets and changes in PLIN2 protein content. Importantly, there was an inverse correlation between changes in PLIN2 protein content and changes in glucose disposal rate (Figure 3C) suggesting that larger, PLIN2 coated lipid droplets may be associated with incomplete lipid oxidation, thus resulting in the accumulation of ceramides and ROS production and disruption of insulin signaling.

Finally, given the observations between lipid droplet size and lipid oxidation as well as that increased lipid oxidation with physical fitness (36), we aimed to determine if physical fitness is related to lipid droplet size. Individuals with higher pre-intervention PAL, METs, and TDEE were protected against a decrease in the number of smaller, peripherally located lipid droplets with eight weeks of overfeeding. Furthermore, a higher content of smaller, peripheral lipid droplets prior to overfeeding was negatively associated with an overfeeding induced weight gain (Figure 5).

One of the limitations of this study, given the translational nature of this investigation, is that our data rests on correlational analyses between lipid droplet size and location within the myofiber and various components of human metabolism. However, this limitation should not by itself make the data that we have presented any less valuable given the fact that all our data is based exclusively in human tissue collected from a clinical investigation. In addition, our study was only performed in healthy men and thus not completely translatable to the population as a whole. We originally aimed to recruit an equal proportion of men and women to our study, but we were not able to recruit and retain enough female participants to this high fat overfeeding study, thus restricted our focus to only male participants. Finally, this study was conducted in healthy individuals without insulin resistance or type 2 diabetes, which could thus limit our understanding to the progressive pathophysiology relating to individuals who already have T2D and still maintain unhealthy eating practices.

Overall, our investigation in lean men indicates that the size and location of lipid droplets, rather than the total IMCL content, is a determinant factor for the magnitude of the increase in insulin resistance and the resistance to weight gain with obesogenic overfeeding. We have shown that smaller, peripherally located lipid droplets are reflective of better physical fitness

and efficient lipid oxidation, which mirrors prior investigations of myofiber lipid droplet location in trained athletes (26). Given the athlete's paradox, whereby highly trained athletes possess large quantities of IMCL and yet possess high insulin sensitivity (2), IMCL alone is not the only culprit behind skeletal muscle insulin resistance. Our data suggest that packaging of lipid into smaller, peripherally located lipid droplets may hold more benefit for improving insulin sensitivity in individuals with type 2 diabetes (Figure 5B). Future investigations should be aimed at remodeling lipid droplet size and location to treat insulin resistance, as well as other factors that regulate lipid droplet size and packaging in relation to lipid oxidation in skeletal muscle.

Supplementary Material

Refer to Web version on PubMed Central for supplementary material.

Acknowledgments

The authors would like to thank Ricardo Rodriguez, Luisa Valverde, Zhengyu Zhang, Clair Cook, Shantele Thomas, Jose Galgani, Virgile Lecoultre, Rob Noland, Jamie LaGrange, Richard Carmouche, Susan Newman, Mindy Gaubert, and Blaine Masinter for their technical assistance. We also want to thank the nursing staff and the research coordinators involved in this overfeeding study. We finally wish to thank all the research volunteers of this study.

Funding Sources: This study was supported by NIH R01-DK060412 (E.R.), K01-DK089005 (D.L.J.) and utilized core facilities at Pennington Biomedical Research Center that are supported in part by NORC (NIH 1P30-DK072476) and COBRE (NIH P20 GM103528) center grants.

References

1. Krssak M, Falk Petersen K, Dresner A, DiPietro L, Vogel SM, Rothman DL, et al. Intramyocellular lipid concentrations are correlated with insulin sensitivity in humans: a 1H NMR spectroscopy study. Diabetologia. 1999; 42:113–116. [PubMed: 10027589]
2. Goodpaster BH, He J, Watkins S, Kelley DE. Skeletal muscle lipid content and insulin resistance: evidence for a paradox in endurance-trained athletes. J Clin Endocrinol Metab. 2001; 86:5755–5761. [PubMed: 11739435]
3. Bajpeyi S, Myrland CK, Covington JD, Obanda D, Cefalu WT, Smith SR, et al. Lipid in skeletal muscle myotubes is associated to the donors' insulin sensitivity and physical activity phenotypes. Obesity (Silver Spring). 2014; 22:426–434. [PubMed: 23818429]
4. Howald H, Hoppeler H, Claassen H, Mathieu O, Straub R. Influences of endurance training on the ultrastructural composition of the different muscle fiber types in humans. Pflugers Archiv : European journal of physiology. 1985; 403:369–376. [PubMed: 4011389]
5. Bajpeyi S, Reed MA, Molskness S, Newton C, Tanner CJ, McCartney JS, et al. Effect of short-term exercise training on intramyocellular lipid content. Appl Physiol Nutr Metab. 2012; 37:822–828. [PubMed: 22691059]
6. Bruce CR, Kriketos AD, Cooney GJ, Hawley JA. Disassociation of muscle triglyceride content and insulin sensitivity after exercise training in patients with Type 2 diabetes. Diabetologia. 2004; 47:23–30. [PubMed: 14673522]
7. Schrauwen-Hinderling VB, Kooi ME, Hesselink MK, Moonen-Kornips E, Schaart G, Mustard KJ, et al. Intramyocellular lipid content and molecular adaptations in response to a 1-week high-fat diet. Obesity research. 2005; 13:2088–2094. [PubMed: 16421342]
8. Bachmann OP, Dahl DB, Brechtel K, Machann J, Haap M, Maier T, et al. Effects of intravenous and dietary lipid challenge on intramyocellular lipid content and the relation with insulin sensitivity in humans. Diabetes. 2001; 50:2579–2584. [PubMed: 11679437]

9. Fabbrini E, Yoshino J, Yoshino M, Magkos F, Tiemann Luecking C, Samovski D, et al. Metabolically normal obese people are protected from adverse effects following weight gain. J Clin Invest. 2015; 125:787–795. [PubMed: 25555214]
10. Klurfeld DM, Kritchevsky D. The Western diet: an examination of its relationship with chronic disease. Journal of the American College of Nutrition. 1986; 5:477–485. [PubMed: 3023470]
11. Briefel RR, McDowell MA, Alaimo K, Caughman CR, Bischof AL, Carroll MD, et al. Total energy intake of the US population: the third National Health and Nutrition Examination Survey, 1988-1991. The American journal of clinical nutrition. 1995; 62:1072S–1080S. [PubMed: 7484924]
12. Johannsen DL, Tchoukalova Y, Tam CS, Covington JD, Xie W, Schwarz JM, et al. Effect of Eight Weeks of Overfeeding on Ectopic Fat Deposition and Insulin Sensitivity: Testing the "Adipose Tissue Expandability" Hypothesis. Diabetes Care. 2014
13. Redman LM, Heilbronn LK, Martin CK, de Jonge L, Williamson DA, Delany JP, et al. Metabolic and behavioral compensations in response to caloric restriction: implications for the maintenance of weight loss. PLoS One. 2009; 4:e4377. [PubMed: 19198647]
14. Lillioja S, Bogardus C. Obesity and insulin resistance: lessons learned from the Pima Indians. Diabetes/metabolism reviews. 1988; 4:517–540. [PubMed: 3061759]
15. Ravussin E, Lillioja S, Anderson TE, Christin L, Bogardus C. Determinants of 24-hour energy expenditure in man. Methods and results using a respiratory chamber. J Clin Invest. 1986; 78:1568–1578. [PubMed: 3782471]
16. Gaster M, Rustan AC, Beck-Nielsen H. Differential utilization of saturated palmitate and unsaturated oleate: evidence from cultured myotubes. Diabetes. 2005; 54:648–656. [PubMed: 15734839]
17. Kovalik JP, Slentz D, Stevens RD, Kraus WE, Houmard JA, Nicoll JB, et al. Metabolic remodeling of human skeletal myocytes by cocultured adipocytes depends on the lipolytic state of the system. Diabetes. 2011; 60:1882–1893. [PubMed: 21602515]
18. Seifert EL, Estey C, Xuan JY, Harper ME. Electron transport chain-dependent and - independent mechanisms of mitochondrial H2O2 emission during long-chain fatty acid oxidation. J Biol Chem. 2010; 285:5748–5758. [PubMed: 20032466]
19. Chappell JB, Perry SV. Biochemical and osmotic properties of skeletal muscle mitochondria. Nature. 1954; 173:1094–1095. [PubMed: 13165721]
20. Seifert EL, Bezaire V, Estey C, Harper ME. Essential role for uncoupling protein-3 in mitochondrial adaptation to fasting but not in fatty acid oxidation or fatty acid anion export. J Biol Chem. 2008; 283:25124–25131. [PubMed: 18628202]
21. Schindelin J, Arganda-Carreras I, Frise E, Kaynig V, Longair M, Pietzsch T, et al. Fiji: an open-source platform for biological-image analysis. Nat Methods. 2012; 9:676–682. [PubMed: 22743772]
22. Obanda DN, Hernandez A, Ribnicky D, Yu Y, Zhang XH, Wang ZQ, et al. Bioactives of Artemisia dracunculus L. mitigate the role of ceramides in attenuating insulin signaling in rat skeletal muscle cells. Diabetes. 2012; 61:597–605. [PubMed: 22315320]
23. Wolins NE, Quaynor BK, Skinner JR, Schoenfish MJ, Tzekov A, Bickel PE. S3-12, Adipophilin, and TIP47 package lipid in adipocytes. J Biol Chem. 2005; 280:19146–19155. [PubMed: 15731108]
24. Stratford S, Hoehn KL, Liu F, Summers SA. Regulation of insulin action by ceramide: dual mechanisms linking ceramide accumulation to the inhibition of Akt/protein kinase B. J Biol Chem. 2004; 279:36608–36615. [PubMed: 15220355]
25. He J, Goodpaster BH, Kelley DE. Effects of weight loss and physical activity on muscle lipid content and droplet size. Obesity research. 2004; 12:761–769. [PubMed: 15166296]
26. van Loon LJ, Koopman R, Manders R, van der Weegen W, van Kranenburg GP, Keizer HA. Intramyocellular lipid content in type 2 diabetes patients compared with overweight sedentary men and highly trained endurance athletes. Am J Physiol Endocrinol Metab. 2004; 287:E558–565. [PubMed: 15165998]
27. MacPherson RE, Herbst EA, Reynolds EJ, Vandenboom R, Roy BD, Peters SJ. Subcellular localization of skeletal muscle lipid droplets and PLIN family proteins OXPAT and ADRP at rest

and following contraction in rat soleus muscle. Am J Physiol Regul Integr Comp Physiol. 2012; 302:R29–36. [PubMed: 22012700]

28. Amati F, Dube JJ, Alvarez-Carnero E, Edreira MM, Chomentowski P, Coen PM, et al. Skeletal muscle triglycerides, diacylglycerols, and ceramides in insulin resistance: another paradox in endurance-trained athletes? Diabetes. 2011; 60:2588–2597. [PubMed: 21873552]
29. Hsieh CT, Chuang JH, Yang WC, Yin Y, Lin Y. Ceramide inhibits insulin-stimulated Akt phosphorylation through activation of Rheb/mTORC1/S6K signaling in skeletal muscle. Cellular signalling. 2014; 26:1400–1408. [PubMed: 24650522]
30. Roy HJ, Lovejoy JC, Keenan MJ, Bray GA, Windhauser MM, Wilson JK. Substrate oxidation and energy expenditure in athletes and nonathletes consuming isoenergetic high- and low-fat diets. The American journal of clinical nutrition. 1998; 67:405–411. [PubMed: 9497183]
31. Barazzoni R, Zanetti M, Gortan Cappellari G, Semolic A, Boschelle M, Codarin E, et al. Fatty acids acutely enhance insulin-induced oxidative stress and cause insulin resistance by increasing mitochondrial reactive oxygen species (ROS) generation and nuclear factor-kappaB inhibitor (IkappaB)-nuclear factor-kappaB (NFkappaB) activation in rat muscle, in the absence of mitochondrial dysfunction. Diabetologia. 2012; 55:773–782. [PubMed: 22159911]
32. Koves TR, Ussher JR, Noland RC, Slentz D, Mosedale M, Ilkayeva O, et al. Mitochondrial overload and incomplete fatty acid oxidation contribute to skeletal muscle insulin resistance. Cell Metab. 2008; 7:45–56. [PubMed: 18177724]
33. Guo Y, Walther TC, Rao M, Stuurman N, Goshima G, Terayama K, et al. Functional genomic screen reveals genes involved in lipid-droplet formation and utilization. Nature. 2008; 453:657–661. [PubMed: 18408709]
34. Covington JD, Noland RC, Hebert RC, Masinter BS, Smith SR, Rustan AC, et al. Perilipin 3 Differentially Regulates Skeletal Muscle Lipid Oxidation in Active, Sedentary and Type 2 Diabetic Males. J Clin Endocrinol Metab. 2015 JC20144125.
35. Bindesboll C, Berg O, Arntsen B, Nebb HI, Dalen KT. Fatty acids regulate perilipin5 in muscle by activating PPARdelta. J Lipid Res. 2013; 54:1949–1963. [PubMed: 23606724]
36. Boon H, Jonkers RA, Koopman R, Blaak EE, Saris WH, Wagenmakers AJ, et al. Substrate source use in older, trained males after decades of endurance training. Medicine and science in sports and exercise. 2007; 39:2160–2170. [PubMed: 18046187]

What is already known about this subject

- Increased content of intramyocellular lipid in skeletal muscle is associated with insulin resistance in individuals with type 2 diabetes
- Alterations in lipid droplet size have been shown in skeletal muscle following weight loss

What this study adds

- Total content of intramyocellular lipid does not change in skeletal muscle after 8 weeks of overfeeding induced weight gain
- Changes in lipid droplet size with weight gain are associated with alterations in insulin sensitivity and lipid oxidation

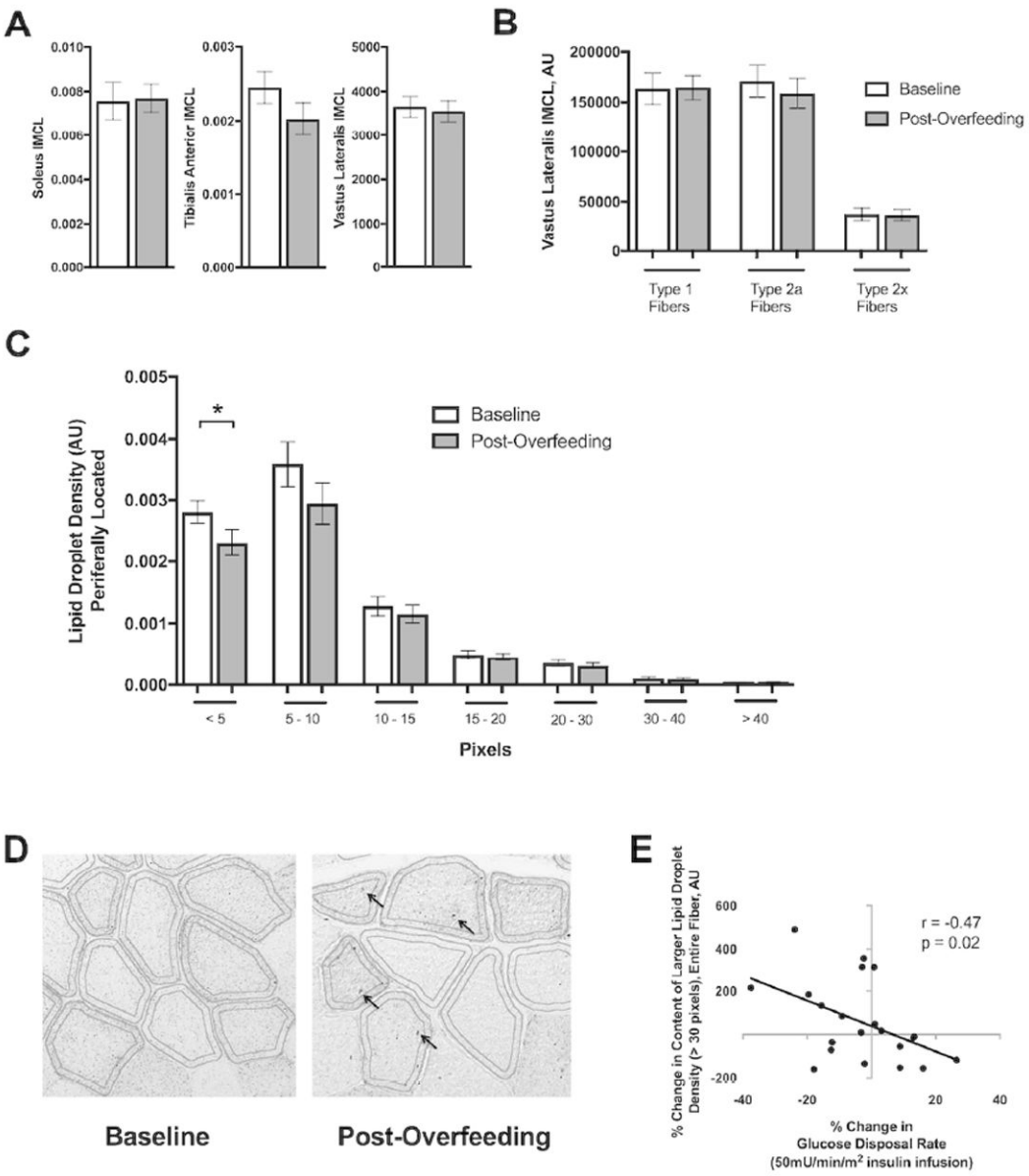

Figure 1. Overfeeding associated increases in the content of large myofiber lipid droplets is related to reductions in insulin sensitivity

A) Total intramyocellular lipid (IMCL) content in the soleus and tibialis anterior via magnetic proton resonance spectroscopy and **B)** in the vastus lateralis using oil red o staining in frozen tissue from biopsy did not increase with overfeeding (N=29 soleus and vastus lateralis, N=28 tibialis anterior). **C)** Lipid droplet size from the vastus lateralis were determined as centrally vs. peripherally located droplets, and the content of small lipid droplets located peripherally decreased (p=0.005, N=25). **D)** Representative image of histological cross-sections of the myofibers stained with oil red o from the same participant before and after overfeeding. Red lined borders indicate the demarcation between central and peripherally location and the outer border of the myofiber. Arrows indicate the large lipid droplets that accumulated with overfeeding in this participant. **E)** Inverse relationship

between the percent change in larger lipid droplets throughout the entire fiber and the percent change in glucose disposal rate (GDR) with overfeeding (r=-0.47, p=0.02, N=23). Graphs represents mean±SEM, *p<0.05.

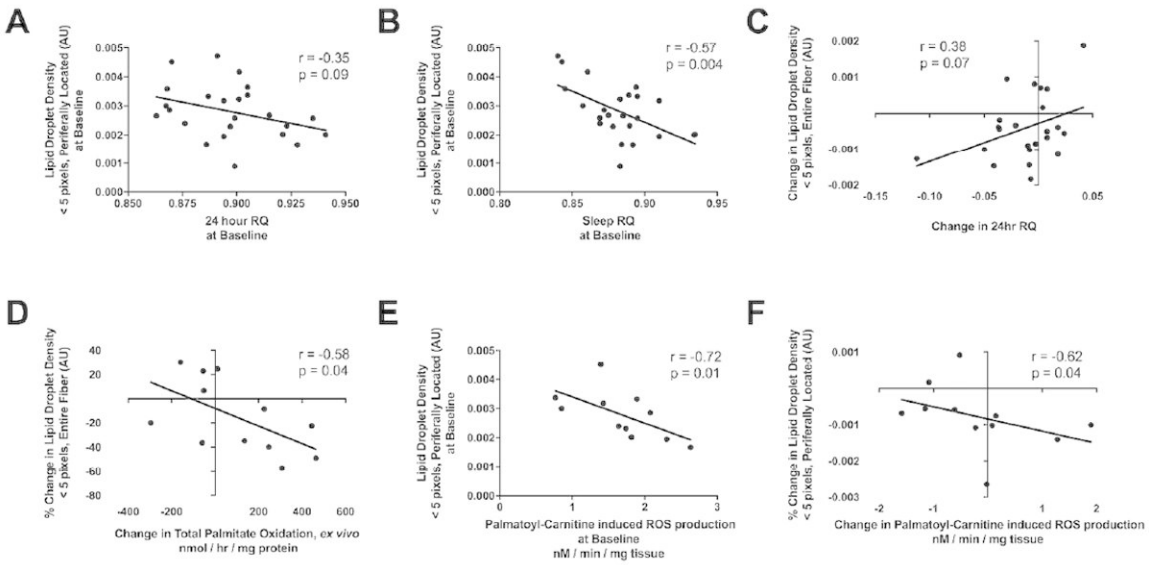

Figure 2. Alterations in lipid droplet size is related to changes in lipid oxidation

A) Baseline content of small, peripherally located lipid droplets are more associated with whole body fat oxidation as evident by inverse relationships with 24 hour respiratory quotient (RQ, r = -0.35, p = 0.09, N = 24) and **B)** sleep RQ (r = -0.57, p = 0.004, N = 24). **C)** Changes in smaller lipid droplet content tended to correlate positively with changes in 24 hr. respiratory quotient (RQ) (r = 0.38, p = 0.07, N = 23), and **D)** correlated inversely to *ex vivo* total palmitate oxidation (r = -0.58, p = 0.04, N = 12). **E)** Smaller, peripherally located lipid droplets at baseline are inversely associated with palmitate produced mitochondrial reactive oxygen species (ROS) production (r = -0.72, p = 0.01, N = 11). **F)** Changes in the content of smaller, peripherally located lipid droplets inversely correlated to changes in palmitate stimulated reactive oxygen species (ROS) production *ex vivo* from isolated mitochondria (r = -0.65, p = 0.03, N = 11).

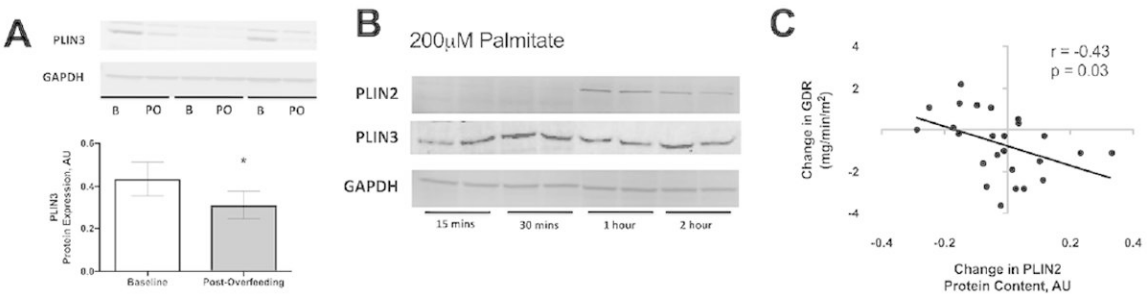

Figure 3. Alterations in lipid droplet size is related to changes in perilipin 2 and perilipin 3 protein expression with overfeeding

A) Perilipin 3 (PLIN3) protein content decreased with overfeeding (p=0.04, N=27). **B)** Baseline human primary myotubes treated with 200μM of palmitate showed that PLIN2 is expressed later over a time course of 2 hours. **C)** Changes in PLIN2 protein content correlated inversely with glucose disposal rate (GDR, r=-0.43, p=0.03, N=25). Graphs represent mean±S.E.M, *p<0.05.

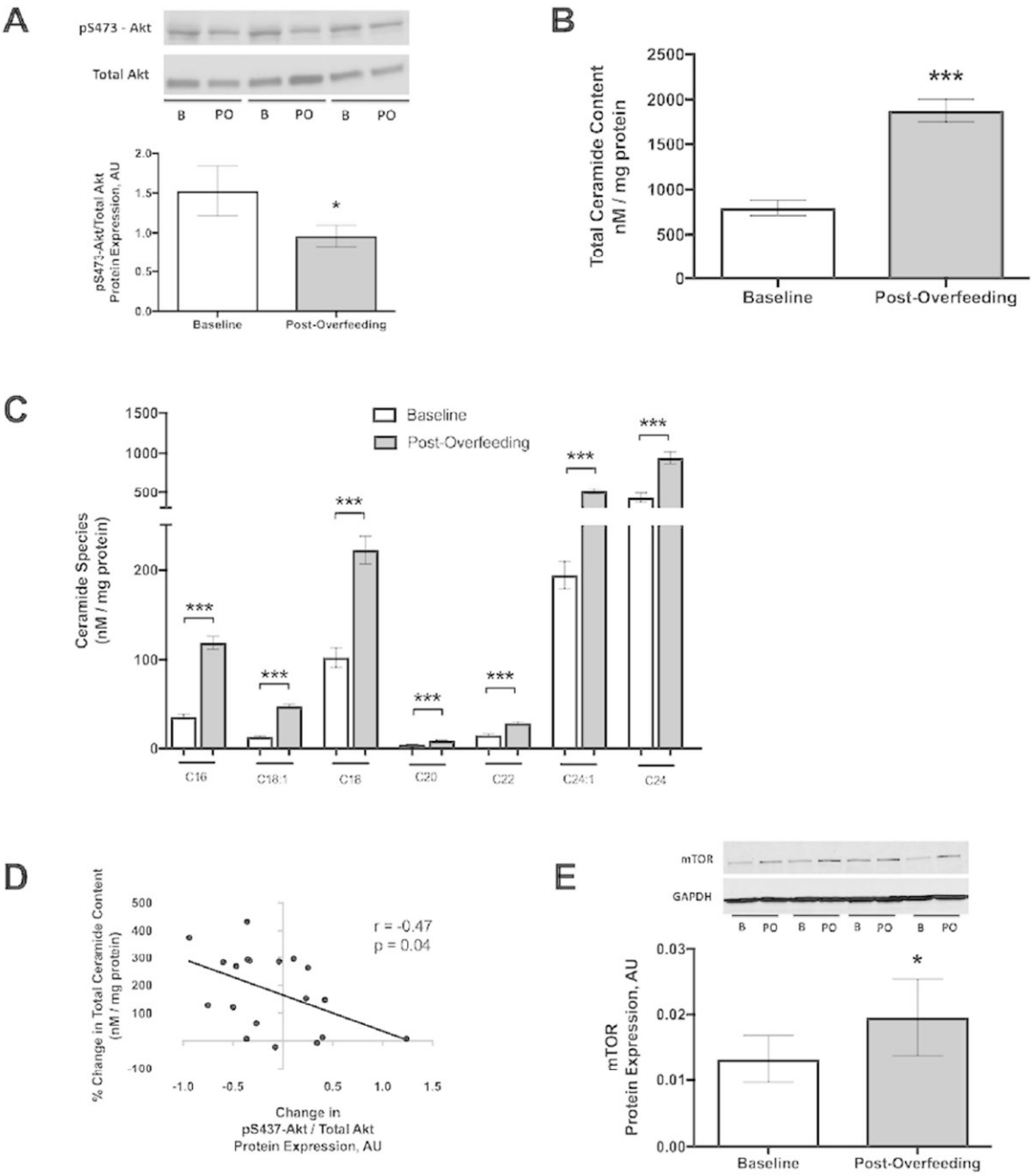

Figure 4. Decreases Akt activity is associated with increased accumulation of ceramide content

A) Decreases in the activity of protein kinase B (PKB/Akt) before and after overfeeding; p=0.05, N=22). **B** and **C)** Muscle total ceramide content and ceramide species increased with overfeeding (p<0.001, all subspecies, N=29). **D)** The percent change in total ceramide content with overfeeding inversely correlated to the change in Akt activity with overfeeding (r=-0.47, p=0.04, N=22). **E)** The protein content of mammalian target of rapamycin (mTOR) increased significantly in skeletal muscle with overfeeding (p=0.05, N=27). Graphs represent mean±S.E.M, *p<0.05; ***p<0.001.

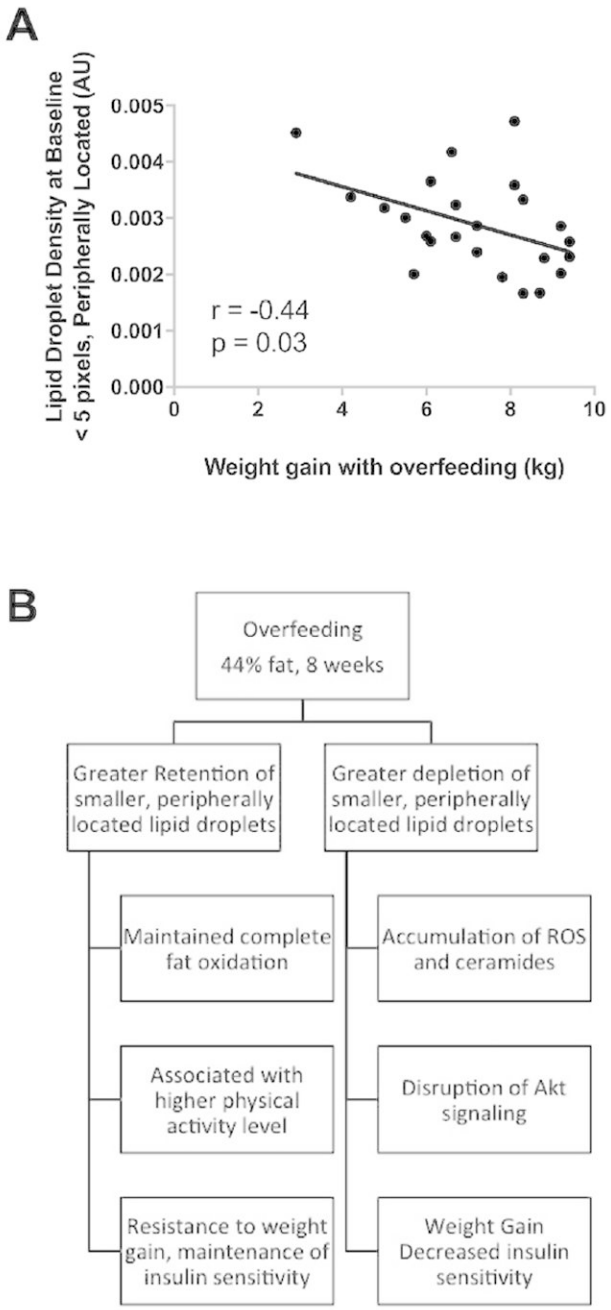

Figure 5. Pre-intervention levels of smaller, peripherally located lipid droplets in muscle was associated with less weight gain during overfeeding

A) Participants who had higher pre-intervention levels of smaller, peripherally located lipid droplets gained less weight with overfeeding, indicating that participants who have smaller, peripherally located lipid droplets are resistant to weight gain with overfeeding (r=-0.44, p=0.03, N=25). **B)** Schematic diagram examining the effects of diet-induced alterations in skeletal muscle lipid droplet morphology.

Table 1

	Baseline Mean ± SD	Post-Overfeeding Mean ± SD
Anthropometric Characteristics		
Weight (kg)	82.8 ± 9.2	89.7 ± 9.4[a]
% Fat	19.7 ± 4.9	22.5 ± 5.2[a]
FM (kg)	16.4 ± 4.8	20.4 ± 5.6[a]
FFM (kg)	66.0 ± 7.4	69.5 ± 7.4[a]
SAT (kg)	4.1 ± 1.4	5.3 ± 1.7[a]
VAT (kg)	0.59 ± 0.50	0.95 ± 0.59[a]
Metabolic Characteristics		
24 hour RQ	0.90 ± 0.02	0.88 ± 0.03[b]
GDR (mg/min/EMBS)	10.92 ± 2.17	10.48 ± 2.39[b]
EGP (mg/min/kg)	0.06 ± 0.16	0.28 ± 0.30[a]
EGP % suppression	96 ± 10	82 ± 20[a]
Serum measures		
Glucose (mg/dL)	90.4 ± 5.2	91.5 ± 7.2
Insulin (μU/mL)	6.6 ± 4.1	7.1 ± 5.2
FFA (nmol/L)	0.27 ± 0.09	0.30 ± 0.10
Triglycerides (mg/dL)	87.3 ± 61.5	100.0 ± 73.0[a]
Total Cholesterol (mg/dL)	176.6 ± 20.9	196.5 ± 30.0[a]
HDL-C (mg/dL)	56.1 ± 13.0	56.9 ± 11.1
LDL-C (mg/dL)	103.1 ± 20.0	119.6 ± 26.4[a]
Cholesterol/HDL	3.34 ± 1.00	3.58 ± 0.93[a]
HDL/LDL	0.57 ± 0.20	0.50 ± 0.16[a]

Study characteristics of the 25 male participants who had lipid droplet analysis performed at baseline and after 8 weeks of overfeeding,

[a] $p<0.05$;

[b] $p<0.10$. FM, fat mass; FFM, fat free mass; SAT, abdominal subcutaneous adipose tissue; VAT, visceral adipose tissue; RQ, respiratory quotient; GDR, glucose disposal rate (from a 50mU/min/m^2 insulin infusion); EGP, endogenous glucose production (n=19); EMBS, estimated mean body size (FFM+17.7); FFA, free fatty acids; HDL, high density lipoprotein cholesterol; LDL, low density lipoprotein cholesterol.